

Heteronuclear inorganic molecule enables the direct synthesis of PtCo intermetallic compounds for proton exchange membrane fuel cells

Bei Liu^{a, b}, Yubin Chen^{a*}, Yanping Zhu^d, Hao Zhao^{a, b}, ShunJie Gui^c, Zhouying Yue^a, Qingqing Cheng^{a*} and Hui Yang^{a, c}

^a Shanghai Advanced Research Institute, Chinese Academy of Sciences, Shanghai, 201210, P. R. China. E-mail: chenlubin@sari.ac.cn, chengqq@sari.ac.cn;

^b University of Chinese Academy of Sciences, Beijing, 100049, P. R. China

^c CAHM Technology (Foshan) Co., Ltd, 528216, P. R. China

^d Ningbo CAS Cotrun New Energy S&T Co., Ltd, 315300, P.R. China

Experimental Procedures

1.1 Chemicals and Materials:

All the chemical reagents were not further purified. Potassium tetrachloroplatinate (II) (K_2PtCl_4) was purchased from Shanghai Haohong Scientific Co., Ltd. Pentaamminechlorocobalt(III) chloride ($[\text{Co}(\text{NH}_3)_5\text{Cl}]\text{Cl}_2$) was purchased from Sigma-Aldrich. Vulcan XC-72 carbon black was purchased from Cabot Corporation. Concentrated perchloric acid (HClO_4) and isopropanol ($\text{C}_3\text{H}_8\text{O}$) were purchased from Sinopharm Chemical Reagent Co., Ltd. The commercial 20% Pt/C catalyst was purchased from Ningbo CASCO Tech New Energy Technology Co., Ltd. The commercial 60% Pt/C catalyst was purchased from Johnson Matthey.

1.2 Synthesis of $[\text{Co}(\text{NH}_3)_5\text{Cl}][\text{PtCl}_4]$:

250 mg of $[\text{Co}(\text{NH}_3)_5\text{Cl}]\text{Cl}_2$ was dissolved in 80 ml of deionized (DI) water. 20 ml of an aqueous solution containing 415 mg K_2PtCl_4 was slowly added into the pre-prepared $[\text{Co}(\text{NH}_3)_5\text{Cl}]\text{Cl}_2$ solution under continuous stirring. The mixture was stirred at room temperature for one day, and the product was filtered and washed three times with DI water. The product was then dried in a vacuum oven at 60 °C overnight.

1.3 Preparation of catalyst:

49 mg of $[\text{Co}(\text{NH}_3)_5\text{Cl}]\text{Cl}_2$ was dissolved in 100 ml of DI water and 200 mg Vulcan XC-72 carbon support was added. After ultrasonic mixing for 30 min, the suspension was vigorously stirred overnight at room temperature. 20 ml of an aqueous solution containing 89 mg K_2PtCl_4 was slowly added to the above mixture under continuous stirring. The mixture was magnetically stirred for several hours at room temperature, the mixture was filtered and dried overnight to obtain the precursors. Subsequently, the dried precursors were thermally treated using a tube furnace. The furnace was then increased to 800 °C at a heating rate of 5 °C/min and hold at this temperature for 1 h and then slowly down to 550 °C for 4 hours under 95% Ar + 5% H_2 . After cooling to room temperature naturally, the obtained powders were washed with 0.5 M H_2SO_4 at 65 °C for 4 h. The acid-treated sample was filtered, washed with DI water for three times and then dried in a vacuum oven at 60 °C overnight to obtain the final catalyst Pt1Co1-IMC/C.

2. Physical characterization:

X-ray diffraction (XRD) patterns were obtained on Bruker D8 ADVANCE X-ray diffractometer with Cu K α radiation. Transmission electron microscopy (TEM) measurements with energy dispersive spectroscopy (EDS) of samples were acquired using a FEI Tal os F200X instrument. Atomic-resolution scanning transmission electron microscopy (STEM) analyses were measured on JEM-ARM300F at 300 kV with a probe aberration corrector. The metal loading of the samples was determined by an inductively coupled plasma optical emission spectroscopy (ICP-OES, America Agilent ICPOES730). X-ray photoelectron spectroscopy (XPS) (Thermo escalab 250XI, America) with an Al K α source was used to characterize the electronic structure of catalysts. The IR spectra of the synthesized heteronuclear molecule were recorded on a Nicolet IS10 FTIR spectrometer (Thermo Nicolet Corporation, the United States).

3. Electrochemical characterization

For all electrochemical measurements, a standard three-electrode system was used on CHI760e electrochemical workstation. The working electrode was a glassy carbon rotating disk electrode (RDE, 5 mm in diameter). A graphite rod and Hg/Hg₂SO₄ were used as the counter and reference electrodes, respectively. All potentials were converted to the reversible hydrogen electrode (RHE) scale.

2 mg of electrocatalyst was dispersed in a mixture containing 975 μ L of isopropanol and 25 μ L of 5 wt % Nafion solution through ultrasonication to form a uniform ink. Subsequently, 13.4 μ L of catalyst ink was dropped onto a precleaned glassy carbon electrode and dried under ambient condition to form a thin film. The final Pt loading of all catalysts was 15 μ g_{Pt}/cm² (determined by ICP-OES).

Cyclic voltammetry (CV) tests were performed in N₂-saturated 0.1 M HClO₄ solution with a scan rate of 50 mV/s between 0.05 - 1.1 V/RHE. The linear sweep voltammetry (LSV) curves were recorded in O₂-saturated 0.1 M HClO₄ solution at a scan rate of 10 mV/s and a rotation speed of 1600 rpm between 0.05 - 1.1 V/RHE. The accelerated durability test (ADT) was conducted at room temperature in a O₂-saturated 0.1 M HClO₄ with a scan rate of 100 mV/s between 0.6 - 1.1 V/RHE .

4. Membrane electrode assemblies (MEAs) tests:

The performance of the catalysts in PEMFCs was tested in a single cell using an Arbin Fuel Cell Testing System (Arbin Instrument Inc, USA). The MEAs were fabricated by catalyst coating membrane (CCM) method. First, an appropriate amount of catalyst was mixed with 5 wt % Nafion solution, deionized water, and isopropanol. The above suspension was ultrasonicated to form a uniform ink for 3 h. Subsequently, the ink was sprayed directly to 12 μm thick ($2.5 \times 2.5 \text{ cm}^2$ active area) Gore membrane at 80 °C by a spray gun. Pt1Co1-IMC/C or 20% Pt/C catalysts were employed as cathode catalysts with the Pt loading of 0.10 $\text{mg}_{\text{Pt}}/\text{cm}^2$. The anode catalysts of all the studied cells were 60% Pt/C with the Pt loading of 0.1 $\text{mg}_{\text{Pt}}/\text{cm}^2$. Steady-state polarization curves of the MEAs were used to examine the practical application potential of the catalysts in PEMFCs under H_2/air or H_2/O_2 conditions. Furthermore, discharging at a constant current density of 1 A cm^{-2} for 100 h was carried out to evaluate the stability. The prepared single cells were all operated at 80 °C with 100 RH% and the back pressure of 1 bar.

5. Computational details:

All calculations were conducted using density functional theory (DFT) method, as implemented in the Vienna *ab initio* Simulation Package (VASP).¹⁻³ The frozen-core projector augmented-wave (PAW) potentials was employed for the core and valence electronic interactions.⁴ The exchange-correlation interaction between electrons was calculated by the general gradient approximation (GGA) function proposed by Perdew-Burke-Ernzerhof (PBE).⁵⁻⁷ The cutoff energy of the plane wave was set as 400 eV. To avoid interactions between periodic slabs, lattice parameters in the direction perpendicular to the surface were set as 25 Å. The van der Waals interaction was calculated using the DFT-D3 method.⁸ The first Brillouin zone was sampled using the Gamma k-point mesh of $2 \times 2 \times 1$. The energy and force convergence criterion were set at 1×10^{-4} eV and 0.01 eV Å⁻¹ per atom, respectively. The formation energies (E_f) were calculated using the equation:

$$E_f = E_{\text{cluster}} + E_{\text{gas molecules}} - E_{\text{precursor}}$$

where E_{cluster} , $E_{\text{gas molecules}}$, and $E_{\text{precursor}}$ are total energies of the graphene substrate

with the absorbed Pt_2Co_2 cluster, the gas molecules and the graphene substrate with the absorbed precursors, respectively.

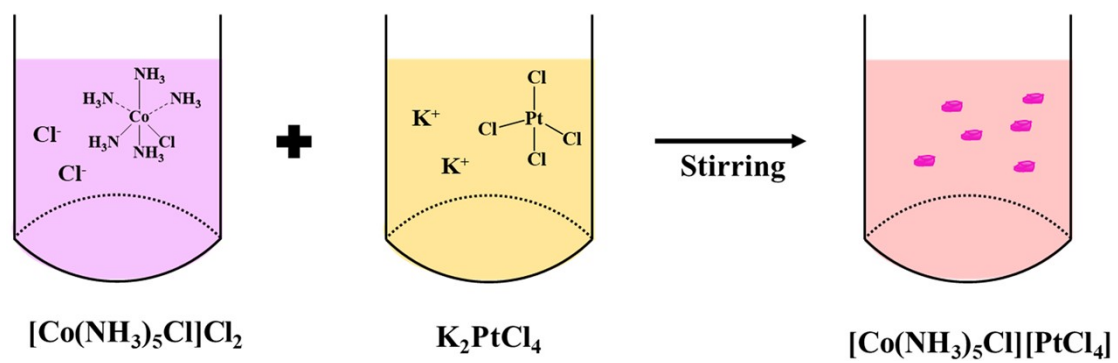


Figure S1. Schematic illustration of the preparation for Pt1Co1-compound.

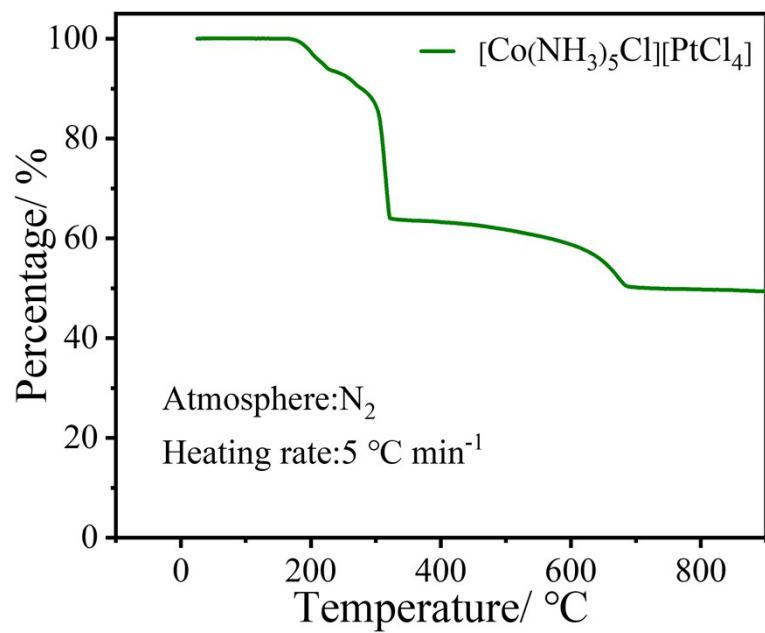


Figure S2. TG curve for the $[\text{Co}(\text{NH}_3)_5\text{Cl}][\text{PtCl}_4]$.

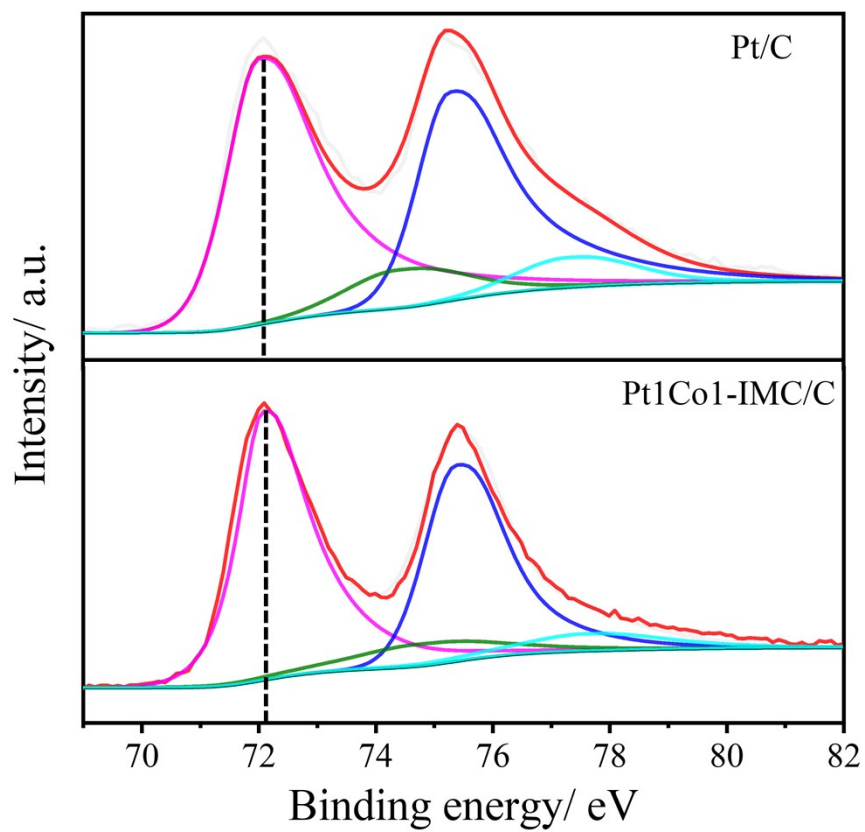


Figure S3. XPS spectra of Pt 4f for Pt/C and Pt1Co1-IMC/C catalysts.

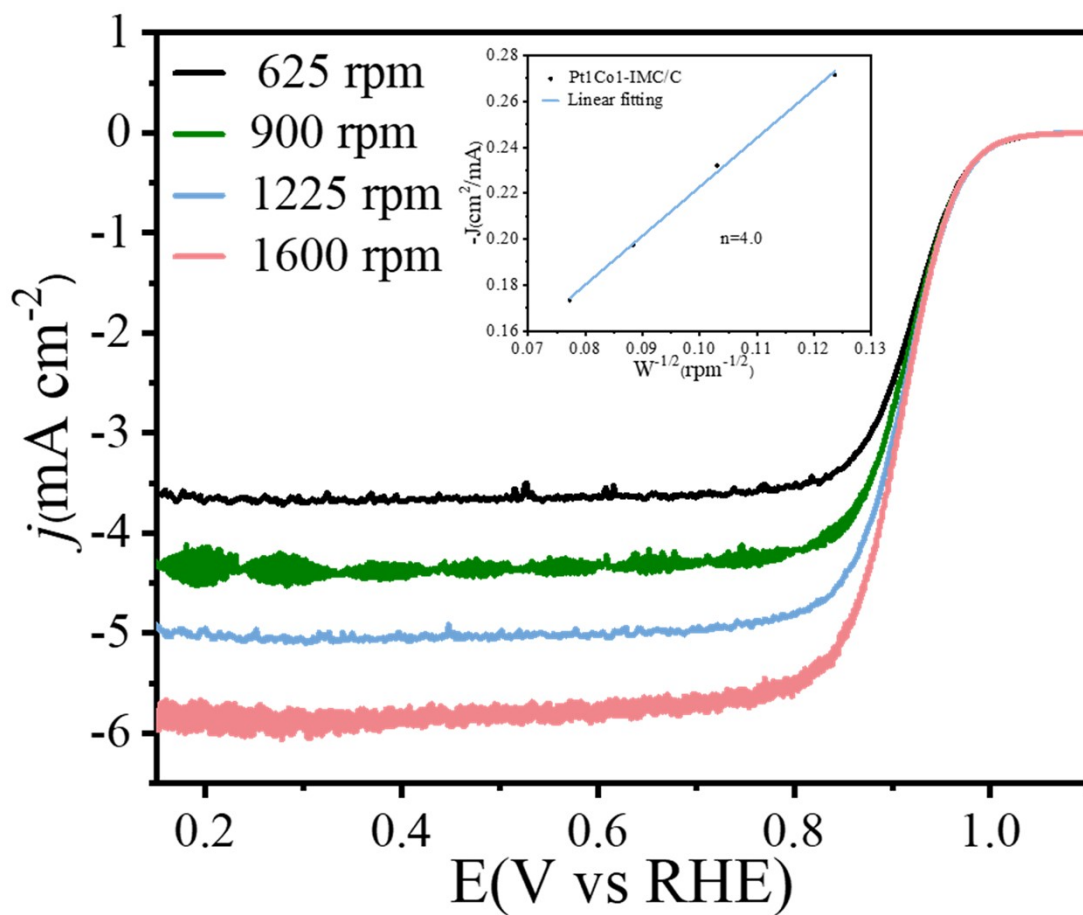


Figure S4. LSV curves at various rotation rates for Pt₁Co₁-IMC/C catalyst, inset is the Koutecky-Levich plot that was obtained at 0.3 V vs. RHE.

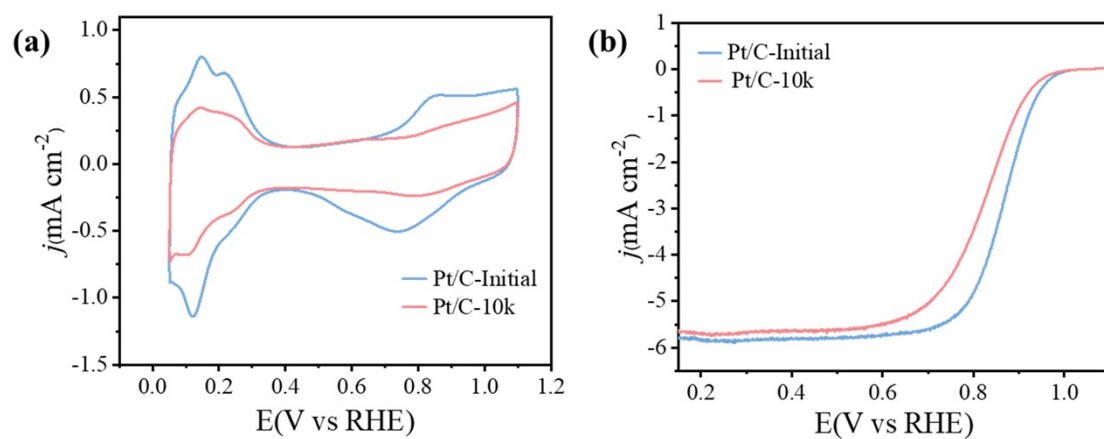


Figure S5. (a) CV and (b) LSV curves before and after ADT for Pt/C.

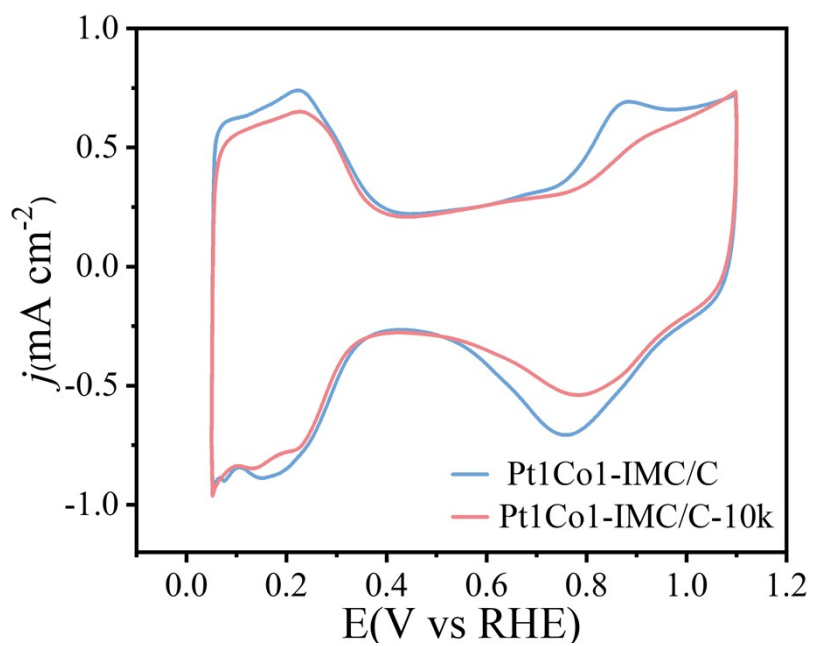


Figure S6. CV curves before and after ADT for Pt1Co1-IMC/C.

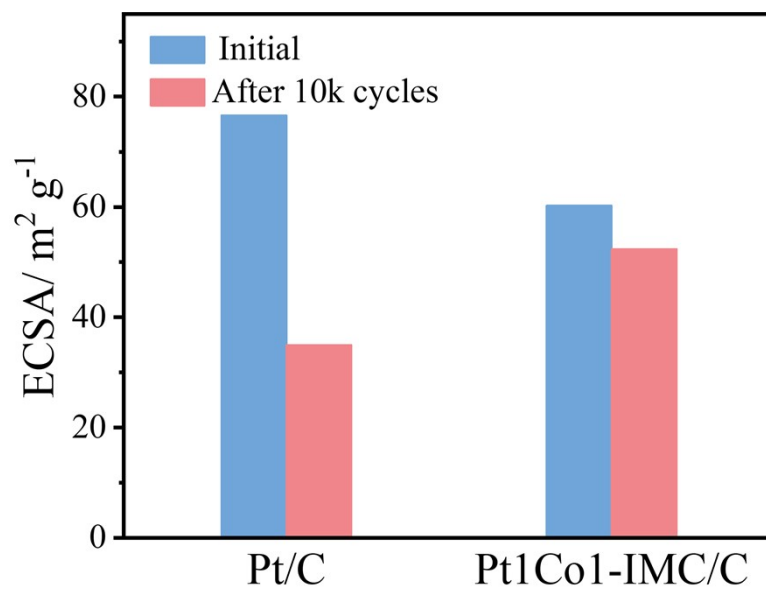


Figure S7. ECSA before and after ADT for Pt1Co1-IMC/C and Pt/C.

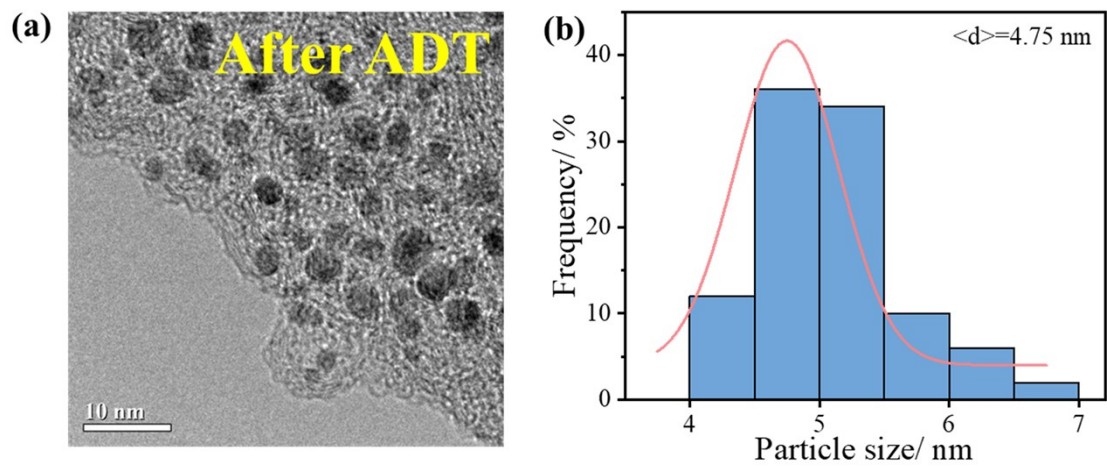


Figure S8. (a) TEM image and (b) size distribution histogram for Pt1Co1-IMC/C after 10 k ADT.

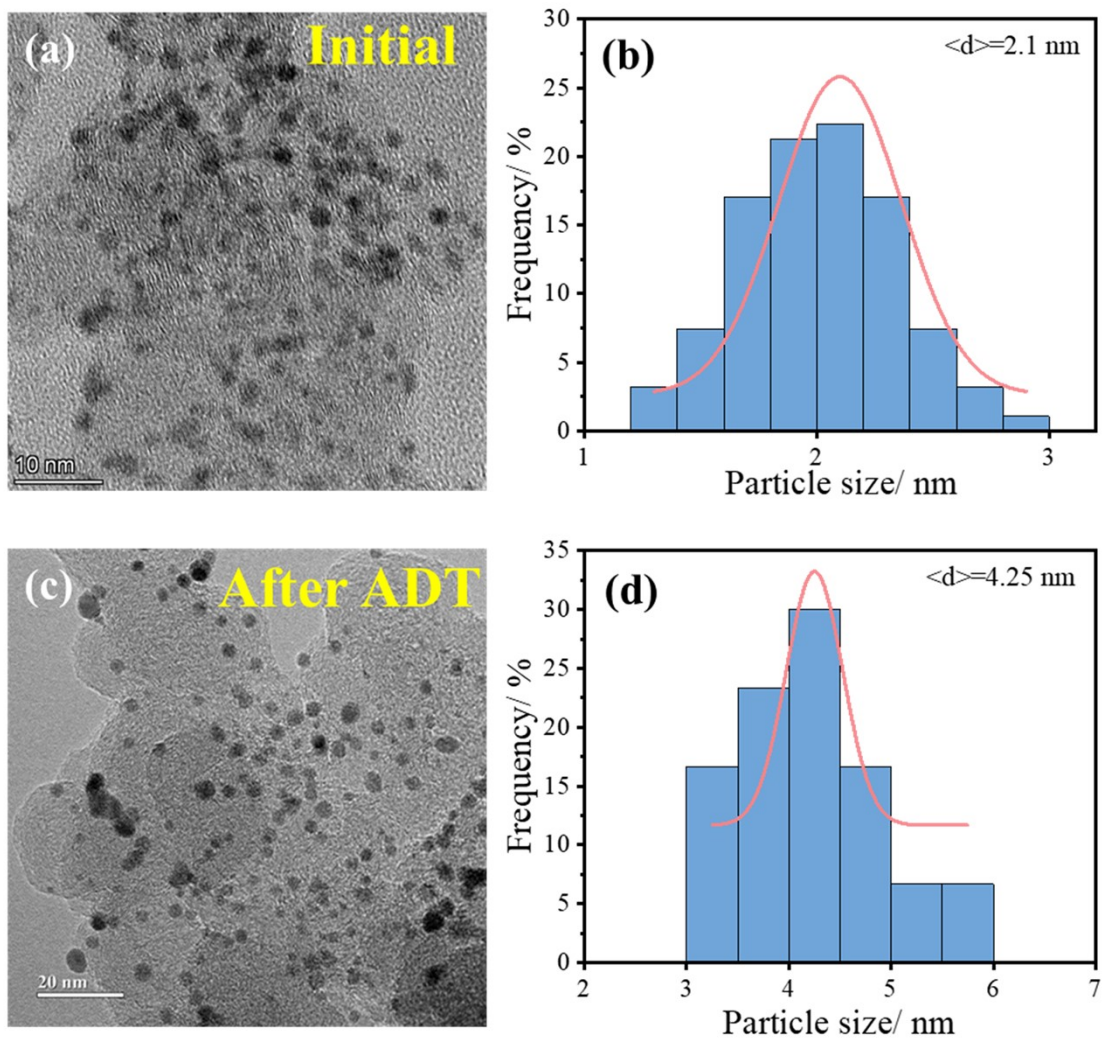


Figure S9. TEM images and size distribution histogram for Pt/C before (a), (b) and after (c), (d) ADT.

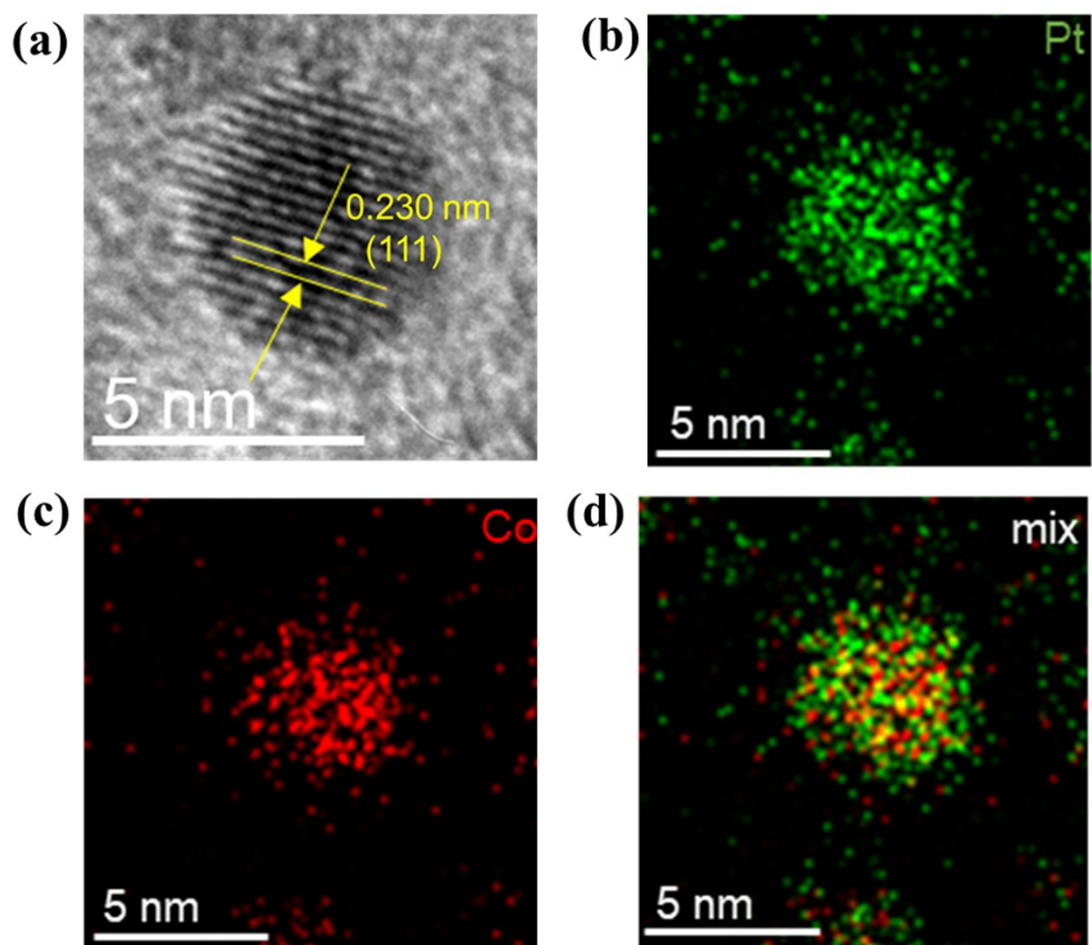


Figure S10. (a) HR-TEM image and (b-d) EDS-mapping for Pt₁Co₁-IMC/C after 10k ADT.

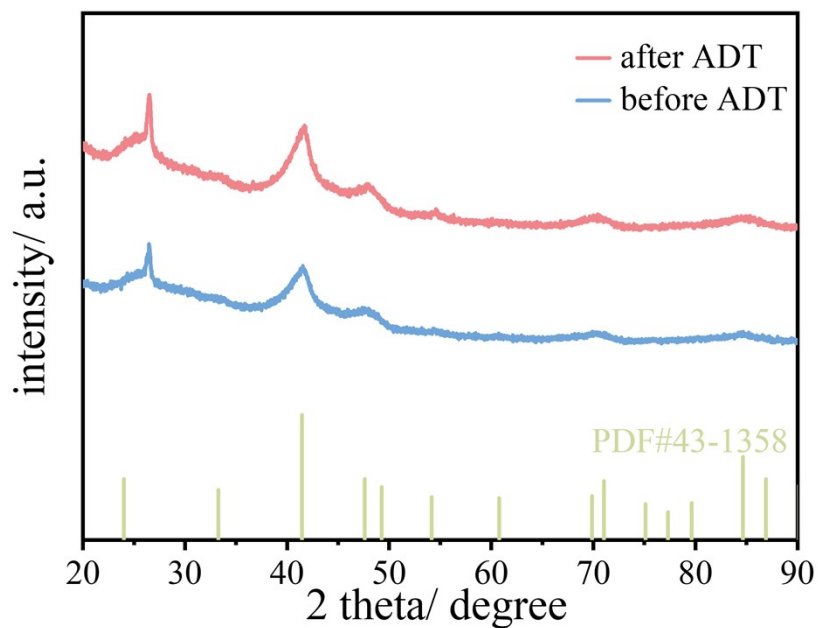


Figure S11. XRD patterns for Pt₁Co₁-IMC/C before and after 10k ADT. (Experimental details: 20 mg of electrocatalyst was dispersed in a mixture containing 1950 μ L of isopropanol and 50 μ L of 5 wt % Nafion solution through ultrasonication to form a uniform ink. Subsequently, the catalyst ink was dropped onto carbon paper and dried under ambient conditions to evaluate the durability of the prepared catalyst. XRD is conducted before and after the ADT to better understand whether the crystal structure of the catalyst has changed.)

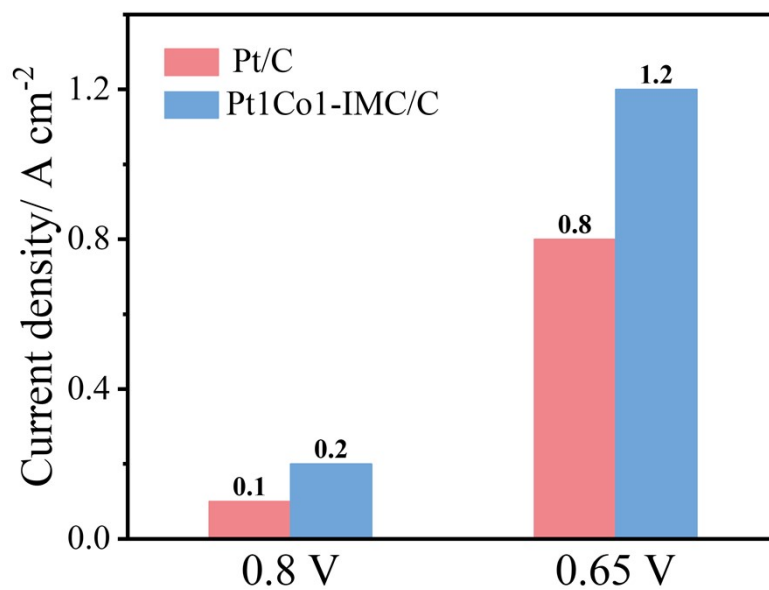


Figure S12. Current density for Pt1Co1-IMC/C (blue) and Pt/C (red) at 0.8 and 0.65 V in the MEA test.

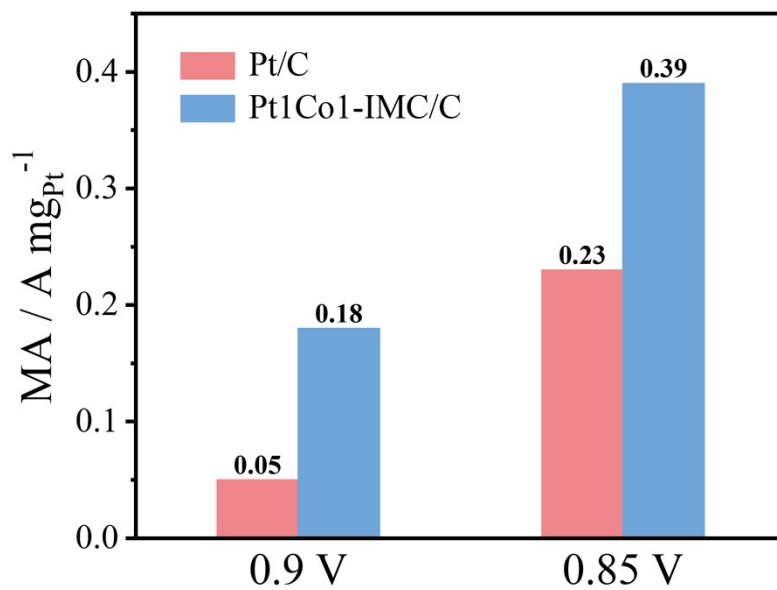


Figure S13. Mass activity for Pt1Co1-IMC/C (blue) and Pt/C (red) at 0.9 and 0.85 V in the MEA test.

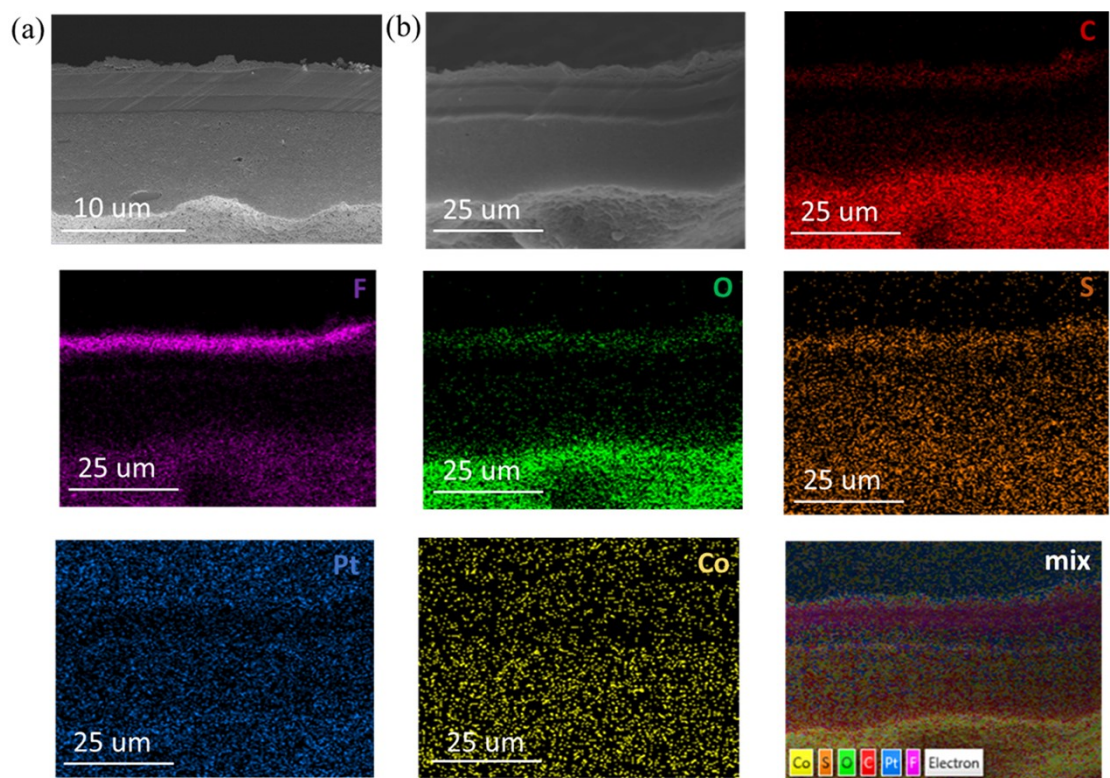


Figure S14. (a) SEM image and (b) EDS-elemental mappings of the cross-section of MEA before the stability test.

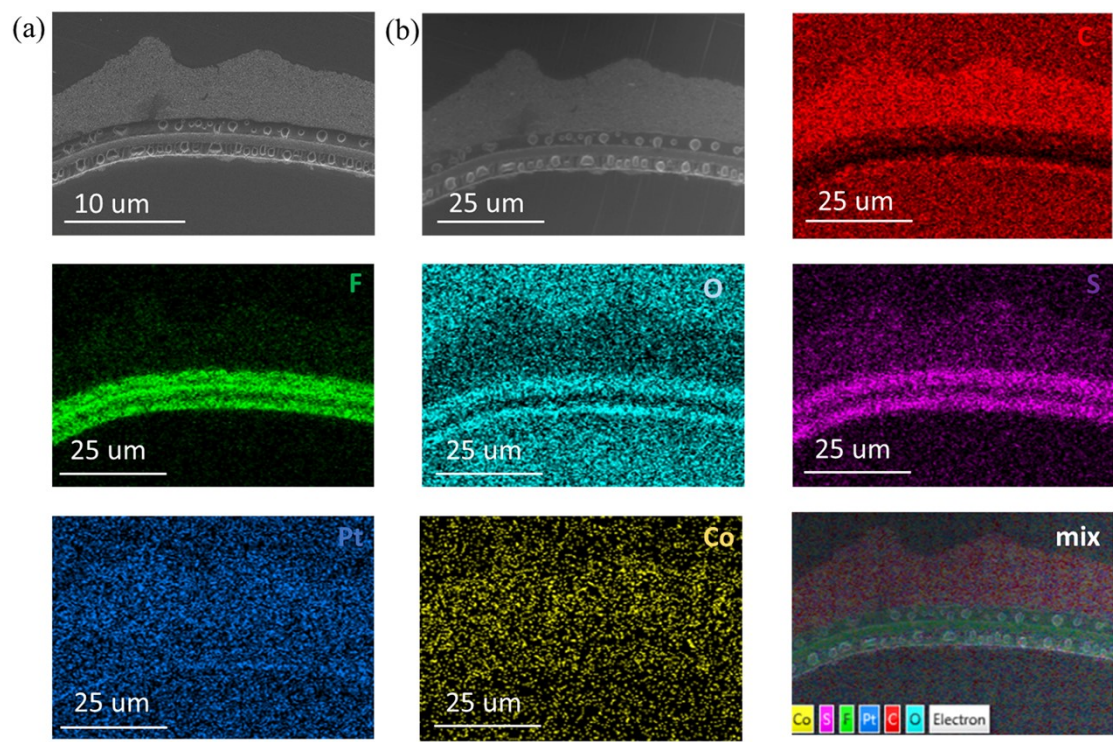


Figure S15. (a) SEM image and (b) EDS-elemental mappings of the cross-section of MEA after the stability test.

Table S1. Bond lengths between metals of different adsorption configurations.

	Co _a -Pt _a	Pt _a -Co _b	Co _a -Pt _b	Pt _b -Co _b	Co _a -Co _b	Pt _a -Pt _b
Configuration a	4.361 Å	5.384 Å	5.471 Å	4.329 Å	7.328 Å	6.544 Å
Configuration b	4.183 Å		5.122 Å	4.414 Å	9.032 Å	5.744 Å
Configuration c	7.425 Å	9.095 Å	7.856 Å	13.422 Å	7.346 Å	6.226 Å
Configuration d	6.673 Å	7.087 Å	5.715 Å	5.889 Å	8.895 Å	6.257 Å

Table S2. The metals content (wt %) for Pt1Co1-compound.

	wt %	wt %(calculated)
Co	11.07	11.4
Pt	37.77	37.7

Table S3. The atomic ratio of Pt and Co for Pt1Co1-compound at various locations.

EDS site	Atomic Pt:Co
#1	56.0:44.0
#2	55.3:44.7
#3	56.3:45.7

Table S4. The performance of H₂-air PEMFCs with advanced Pt-based catalysts as cathode.

Catalyst	Test condition			Peak power density/W cm ⁻²	Current density @0.65 V /A cm ⁻²	Reference
	Temperature	Back pressure	Loading cathode (mg _{Pt} cm ⁻²)			
Pt1Co1-IMC/C	80 °C	1 bar	0.10	1.06	1.2	This work
PtCo/NGC	80 °C	170 kPa	0.1	0.697	~0.75	9
Pt67Co31W2	80 °C	150 kPa	0.11	~0.6	~0.81	10
L1 ₀ -PtZn/Pt-C	80 °C	150 kPa	0.104	~0.8	~1.18	11
PtCo i-NPs	80 °C	250 kPa	0.02	1.08	~1.20	12
PtCo/KB-NH ₂	80 °C	150 kPa	0.1	0.96	~1.54	13
L1 ₂ -Pt ₃ Co@ML-Pt/NPC ₁₀	80 °C	1 bar	0.2	~1.02	~1.3	14
ftc-PtCo@Co-N-C	70 °C	30 psi	0.1	0.8	~1.12	15
L1 ₀ -CoPt	80 °C	100 kPa	\	0.895	~1.04	16
PtCo@Gnp	80 °C	150 kPa	0.1	1.01	1.45	17
P _{NS} -Pt/C	80 °C	50 kPa	0.15	1.06	0.15	18

References

1. Kresse and Hafner, *Phys. Rev. B*, 1993, **48**, 13115-13118.
2. G. Kresse and J. Furthmüller, *Comput. Mater. Sci*, 1996, **6**, 15-50.
3. Kresse and Furthmüller, *Phys. Rev. B*, 1996, **54**, 11169-11186.
4. Blochl, *Phys. Rev. B*, 1994, **50**, 17953-17979.
5. Perdew and Wang, *Phys. Rev. B*, 1992, **45**, 13244-13249.
6. Perdew, Chevary, Vosko, Jackson, Pederson, Singh and Fiolhais, *Phys. Rev. B*, 1992, **46**, 6671-6687.
7. Perdew, Burke and Wang, *Phys. Rev. B*, 1996, **54**, 16533-16539.
8. S. Grimme, S. Ehrlich and L. Goerigk, *J. Comput. Chem.*, 2011, **32**, 1456-1465.
9. W. S. Jung, W. H. Lee, H.-S. Oh and B. N. Popov, *Journal of Materials Chemistry A*, 2020, **8**, 19833-19842.
10. J. Liang, N. Li, Z. Zhao, L. Ma, X. Wang, S. Li, X. Liu, T. Wang, Y. Du, G. Lu, J. Han, Y. Huang, D. Su and Q. Li, *Angewandte Chemie International Edition*, 2019, **58**, 15471-15477.
11. J. Liang, Z. Zhao, N. Li, X. Wang, S. Li, X. Liu, T. Wang, G. Lu, D. Wang, B. J. Hwang, Y. Huang, D. Su and Q. Li, *Advanced Energy Materials*, 2020, **10**, 2000179.
12. C.-L. Yang, L.-N. Wang, P. Yin, J. Liu, M.-X. Chen, Q.-Q. Yan, Z.-S. Wang, S.-L. Xu, S.-Q. Chu, C. Cui, H. Ju, J. Zhu, Y. Lin, J. Shui and H.-W. Liang, *Science*, 2021, **374**, 459-464.
13. Q. Gong, H. Zhang, H. Yu, S. Jeon, Y. Ren, Z. Yang, C.-J. Sun, E. A. Stach, A. C. Foucher, Y. Yu, M. Smart, G. M. Filippelli, D. A. Cullen, P. Liu and J. Xie, *Matter*, 2023, **6**, 963-982.
14. Z. Wang, S. Chen, W. Wu, R. Chen, Y. Zhu, H. Jiang, L. Yu and N. Cheng, *Advanced Materials*, 2023, **35**, 2301310.
15. J. Chen, J. Dong, J. Huo, C. Li, L. Du, Z. Cui and S. Liao, *Small*, 2023, **19**, 2301337.
16. J. Guan, J. Zhang, X. Wang, Z. Zhang and F. Wang, *Advanced Materials*, 2022, **35**, 2207995.
17. Z. Zhao, Z. Liu, A. Zhang, X. Yan, W. Xue, B. Peng, H. L. Xin, X. Pan, X. Duan and Y. Huang, *Nature Nanotechnology*, 2022, **17**, 968-975.
18. B.-A. Lu, L.-F. Shen, J. Liu, Q. Zhang, L.-Y. Wan, D. J. Morris, R.-X. Wang, Z.-Y. Zhou, G. Li, T. Sheng, L. Gu, P. Zhang, N. Tian and S.-G. Sun, *ACS Catalysis*, 2020, **11**, 355-363.